Journal of Visualized Experiments

Cooling an optically-trapped ultracold Fermi gas by periodical driving

--Manuscript Draft--

Manuscript Number:	JoVE55409R3
Full Title:	Cooling an optically-trapped ultracold Fermi gas by periodical driving
Article Type:	Invited Methods Article - JoVE Produced Video
Keywords:	Laser Cooling; Laser Trapping; Ultracold Atoms; Optical Dipole Trap; Parametric Cooling; Degenerate Fermi Gas
Manuscript Classifications:	97.72: Atomic and Molecular Physics; 97.74: Optics
Corresponding Author:	Le Luo, Ph.D. Indiana University Purdue University at Indianapolis Indianapolis, Indiana UNITED STATES
Corresponding Author Secondary Information:	
Corresponding Author E-Mail:	leluo@iupui.edu
Corresponding Author's Institution:	Indiana University Purdue University at Indianapolis
Corresponding Author's Secondary Institution:	
First Author:	Jiaming Li
First Author Secondary Information:	
Other Authors:	Jiaming Li
	Leonardo de Melo
Order of Authors Secondary Information:	
Abstract:	We present a cooling method for a cold Fermi gas by parametrically driving atomic motions in a crossed-beam optical dipole trap (ODT). Our method employs the anharmonicity of the ODT, in which the hotter atoms at the edge of the trap feel the anharmonic components of the trapping potential, while the colder atoms in the center of the trap feel the harmonic one. By modulating the trap depth with frequencies that are resonant with the anharmonic components, we selectively excite the hotter atoms out of the trap while keeping the colder atoms in the trap, generating parametric cooling. This experimental protocol starts with a magneto-optical trap (MOT) that is loaded by a Zeeman slower. The precooled atoms in the MOT are then transferred to an ODT, and a bias magnetic field is applied to create an interacting Fermi gas. We then lower the trapping potential to prepare a cold Fermi gas near the degenerate temperature. After that, we sweep the magnetic field to the noninteracting regime of the Fermi gas, in which the parametric cooling can be manifested by modulating the intensity of the optical trapping beams. We find that the parametric cooling effect strongly depends on the modulation frequencies and amplitudes. With the optimized frequency and amplitude, we measure the dependence of the cloud energy on the modulation time. We observe that the cloud energy is changed in an anisotropic way, where the energy of the axial direction is significantly reduced by parametric driving. The cooling effect is limited to the axial direction because the dominant anharmonicity of the crossed-beam ODT is along the axial direction. Finally, we propose to extend this protocol for the trapping potentials of large anharmonicity in all directions, which provides a promising scheme for cooling quantum gases using external driving.
Author Comments:	
Additional Information:	
Question	**Response**
If this article needs to be "in-press" by a certain date, please indicate the date	

below and explain in your cover letter.	

TITLE:
Cooling an optically-trapped ultracold Fermi gas by periodical driving

AUTHORS:
Li, Jiaming
Department of Physics
Indiana University Purdue University Indianapolis (IUPUI)
Indianapolis, IN, USA
jiamli@iupui.edu

de Melo, Leonardo, F.
Department of Physics
Indiana University Purdue University Indianapolis (IUPUI)
Indianapolis, IN, USA
ldemelo@iupui.edu

Luo, Le
Department of Physics
Indiana University Purdue University Indianapolis (IUPUI)
Indianapolis, IN, USA
leluo@iupui.edu

CORRESPONDING AUTHOR:
Le Luo (leluo@iupui.edu)

KEYWORDS:
Laser Cooling, Laser Trapping, Ultracold Atoms, Optical Dipole Trap, Parametric Cooling, Degenerate Fermi Gas

SHORT ABSTRACT:
We present a parametric driving method to cool an ultracold Fermi gas in a crossed-beam optical dipole trap. This method selectively removes high-energy atoms from the trap by periodically modulating the trap depth with frequencies that are resonant with the anharmonic components of the trapping potential.

LONG ABSTRACT:
We present a cooling method for a cold Fermi gas by parametrically driving atomic motions in a crossed-beam optical dipole trap (ODT). Our method employs the anharmonicity of the ODT, in which the hotter atoms at the edge of the trap feel the anharmonic components of the trapping potential, while the colder atoms in the center of the trap feel the harmonic one. By modulating the trap depth with frequencies that are resonant with the anharmonic components, we selectively excite the hotter atoms out of the trap while keeping the colder atoms in the trap, generating parametric cooling. This experimental protocol starts with a magneto-optical trap (MOT) that is loaded by a Zeeman slower. The precooled atoms in the MOT are then

transferred to an ODT, and a bias magnetic field is applied to create an interacting Fermi gas. We then lower the trapping potential to prepare a cold Fermi gas near the degenerate temperature. After that, we sweep the magnetic field to the noninteracting regime of the Fermi gas, in which the parametric cooling can be manifested by modulating the intensity of the optical trapping beams. We find that the parametric cooling effect strongly depends on the modulation frequencies and amplitudes. With the optimized frequency and amplitude, we measure the dependence of the cloud energy on the modulation time. We observe that the cloud energy is changed in an anisotropic way, where the energy of the axial direction is significantly reduced by parametric driving. The cooling effect is limited to the axial direction because the dominant anharmonicity of the crossed-beam ODT is along the axial direction. Finally, we propose to extend this protocol for the trapping potentials of large anharmonicity in all directions, which provides a promising scheme for cooling quantum gases using external driving.

INTRODUCTION:

In the past two decades, various cooling techniques have been developed for generating Bose-Einstein condensates (BEC) and degenerate Fermi gases (DFG) from hot atomic vapors[1-5]. BEC and DFG are novel phases of matter that exist in extremely low temperatures, usually one millionth of a degree above absolute zero temperature, far below those normally found on Earth or in space. To obtain such low temperatures, most cooling methods rely on lowering the trapping potential to evaporatively cool the atoms. However, the lowering scheme also decreases the collision rate of the atoms, which limits the cooling efficiency when the gas reaches the quantum regime[6]. In this article, we present an “expelling” method to evaporatively cool an ultracold Fermi gas in an ODT without lowering the trap depth. This method is based on our recent study of parametric cooling[7], showing several advantages compared to the lowering schemes[7-9].

The key idea of the parametric scheme is to employ the anharmonicity of the crossed-beam ODT, which makes the hotter atoms near the edge of the trapping potential feel the lower trapping frequencies than the colder atoms in the center. This anharmonicity allows the hotter atoms to be selectively expelled from the trap when modulating the trapping potential at frequencies resonant with the high-energy atoms.

The experimental protocol of parametric cooling requires a pre-cooled noninteracting Fermi gas near the degenerate temperature. To implement this protocol, an acousto-optic modulator (AOM) is used to modulate the intensity of the trapping beams by controlling the modulation frequency, depth and time. To verify the cooling effect, the atomic cloud is probed by absorption imaging of time-of-flight (TOF), where a resonant laser beam illuminates the atomic cloud and the absorption shadow is captured by a charge coupled device (CCD) camera. The cloud properties, such as the atom number, energy, and temperature, are determined by the column density. To characterize the cooling effect, we measure the dependence of the cloud energies on the various modulation times.

PROTOCOL:

Note: This protocol requires a home-built ultracold atom apparatus including the following equipment: two external cavity diode lasers (ECDL), a locking setup for the ECDL offset frequency locking[10], a fiber laser for the ODT, an AOM for laser intensity modulation, an radio frequency (rf) antenna system with a source generator and a power amplifier, an absorption imaging system with a CCD camera, a computer program for timing sequence and data acquisition (DAQ), a computer program for imaging processing and data analysis, a pair of electromagnets for the MOT and bias magnetic fields, and an ultrahigh vacuum chamber including a ^{6}Li vapor oven and a Zeeman slower (shown in Figure 1).

Caution: Three lasers of different powers and wavelengths are used. Please consult the relevant laser safety data sheets and choose the proper laser safety goggles.

1. Timing Control

Note: All timing sequences are controlled by a 128 channel PCI DAQ card through a timing control program. The resolution of the timing sequence is 100 µs. Several instrumentation control programs are used to control the settings of the instruments, such as fiber laser arbitrary function generator (AFG), ODT AFG, arbitrary pulse generator (APG), parametric modulation AFG, MOT multiplexer, rf generator, *etc*.

1.1. Open the timing control program and the control programs for the instruments.

Note: The timing control program sends TTL (Transistor-transistor logic) signals to the control terminals for running the timing control files. Some instruments are connected to the computer by GPIB (IEEE 488) for real-time control.

1.2. Write the experiment timing file and set the timing parameters as listed in Table 1.

Note: The after MOT timing sequence is also illustrated by Figure 2.

2. CCD Camera Preparation

Note: CCD camera is used to record the absorption imaging of the cold atoms, which is the main diagnostic tool of cold atoms.

2.1. Turn on the CCD camera driver and its control program. Set the CCD camera to Particle image velocimetry (PIV) mode[11]. Set the CCD exposure time to 5 ms.

Note: PIV mode reduces the time gap between the signal and reference frame, which increases the signal-to-noise ratio of the absorption imaging.

2.2. Use an external trigger to control the CCD exposure

Note: The CCD trigger time is listed in Table 1.

3. 671 nm Laser Preparation

Note: A 671 nm single frequency ECDL with 500 mW output power is used to generate the MOT cooling and trapping beams. Another 671 nm ECDL of 35 mW is used for absorption imaging. A digital laser current modulation method (DLCM) is applied for laser frequency stabilization[10]. The related ^{6}Li energy levels are shown in Figure 3a. Room temperature stability of 20 ± 1 °C is required for the optimal stability of laser frequency locking.

3.1. MOT Laser Preparation

Note: The optical setup and relevant results of the DLCM method is presented in Reference 10.

3.1.1. Turn on the ^{6}Li atomic vapor cell heater and warm it up to 340 °C.

3.1.2. Warm up the laser locking AOM for 1 h.

3.1.3. Turn on the laser frequency lock controller and open its software. Turn on the laser grating and current modulation of the ECDL in the software.

Note: The modulation frequency and amplitude of the grating modulation are set to 5 Hz and 1.0 V respectively. The modulation frequency and amplitude of the current modulation are set to 100 kHz and 0.0015 V_{pp} respectively to reduce the laser linewidth[10].

3.1.4. Turn on the ECDL emission.

Note: The laser light passes through the MOT optical setup and reaches the experiment vacuum chamber.

3.1.5. Slightly adjust the current of the ECDL laser manually to tune the laser frequency until the lock-in error signal of the ^{6}Li D_2 line is observed, as shown in Figure 3b.

3.1.6. Set the lock point in the control software to the $2^2S_{1/2}$ (F = 3/2) $\rightarrow$ $2^2P_{3/2}$ transition (see Figures 3a, 3b). Then lock the laser frequency to this transition, and adjust the lock point to the center of the transition[10].

Note: Once the laser frequency is locked, the lock-in error signal shows a small fluctuation at the lock point corresponding to the frequency fluctuation around the lock point.

3.2. Imaging Laser Preparation

Note: The optical setup and relevant results of the offset locking method are presented in Reference 10.

3.2.1. Turn on the offset locking rf signal generator.

3.2.2. Turn on the modulation of the grating, and increase the modulation amplitude to 2 V.

3.2.3. Repeat the frequency tuning process in 3.1.4.-3.1.5. to get the laser frequency beating error signal in the oscilloscope and the rf spectrum analyzer.

3.2.4. Lock the laser frequency to the beating signal of the offset locking through two PID feedback modules.

Note: Once the laser frequency is locked, the spectrum of the beating signal in the rf spectrum will stop at the locking point.

4. Absorption Imaging Preparation

Note: The atoms are probed with absorption imaging, which needs two image frames. The first one with the atoms is the signal frame, and the second one without atoms is the reference frame.

4.1. Turn on an APG and the imaging beam AOM.

4.2. Set the imaging pulse duration to 10 µs, and set the separation time between the two imaging frames to 5.5 ms.

4.3. Set the imaging beam intensity to about $0.3I_{sat}$, where I_{sat} = 2.54 mW/cm^2 is the saturated absorption intensity of the ^{6}Li D_2 line.

5. Cooling Atoms with MOT

Note: MOT is a widely-used cooling method in ultracold atoms experiments. This section generates a MOT of around one billion ^{6}Li atoms at about 300 µK.

5.1. Slow Atom Source

5.1.1. Turn on the oven heaters.

5.1.2. After the oven temperatures reach the operational region (refer to Table 2), turn on the cooling fans for the Zeeman slower. Then slowly increase the current of the slower to 9.2 A. Turn on the current of the two crossover coils to 7 A and 1 A respectively.

Note: The temperature distribution of the oven listed in Table 2 is optimized for collimation and lifetime of the atomic source[12].The location of the heaters on the oven is shown in Figure 4.

5.1.3. Unblock the Zeeman slower laser beam manually by opening the atomic shutter. Set the frequency of the laser beam to 192 MHz red-detuned with the $2^2S_{1/2}$ (F = 3/2) → $2^2P_{3/2}$ transition.

Note: With this setup, the speed of the atoms is slowed down from 1400 m/s to 100 m/s. The Zeeman slower is shown in Figure 5.

5.2. Magnetic Field Gradient

Note: This apparatus uses a pair of coils controlled by an H-bridge switch circuit to produce either an anti-Helmholtz or Helmholtz magnetic field. The coils are water cooled to prevent overheating.

5.2.1. Slowly turn on the water flow to 6 gal/min.

5.2.2. Set the H-bridge for anti-Helmholtz magnetic field configuration by running the timing control program with the MOT loading timing file.

5.2.3. Turn on the magnets' power supplies, and set the current of each coil to about 18 A via its control program, which creates a magnetic field gradient of about 22 G/cm for the MOT.

Note: A static MOT is observed in the experiment chamber after the magnetic field gradient is turned on.

5.3. Dynamic MOT

Note: The optical setup of the ^{6}Li MOT contains three pairs of counter propagating MOT beams with all pairs orthogonal to each other. Each MOT beam includes a cooling beam and a repumping beam. The intensities and frequency detunings of the beams, which are controlled by AOMs, are varied for the three phases. The control voltages of the AOMs are set via multiplexer circuits commanded by a timing control system. The parameters for three phases are listed in Table 3. The optical layout of the MOT beams is shown in Figure 6.

5.3.1. Load, compile and run the experiment timing file in the timing control program on a loop with the software control. The experiment timing starts with the MOT loading phase. Monitor the MOT fluorescence signal in the photodetector to reach 2 V, which indicates around 10^9 atoms in the MOT.

Note: The fluorescence of the MOT is collected by a lens with spatial angle of about 10^{-4} rad. The loading phase atom number can be calculated by the method in Reference 13.

5.3.2. Use the optical shutter to block the slowing beam before the loading phase ends.

Note: The timing of the slowing beam shutter is also under control of the experiment timing, which is listed in Table 1.

5.3.3. Set intensities and frequency detunings of the MOT laser beams according to Table 3 for the cooling phase.

Note: After the cooling phase, the temperature of the MOT is reduced to about 300 μK.

5.3.4. For the pumping phase, program the experiment timing file to turn off the repumping beams with the AOM.

Note: The pumping phase pumps all the atoms into the lowest hyperfine states $2^2S_{1/2}$ ($F = 1/2$).

5.3.5. Turn off the MOT beams and shift the laser frequency 30 MHz below the atomic transition resonance by AOM, and block the leaking light from the AOMs with optical shutters.

Note: After the MOT stage, any leakage of the resonant light to the atomic cloud will result in atom loss. The timing of the AOM control and MOT beam shutter are all listed in Table 1.

5.3.6. After the dynamic MOT, acquire the imaging frames from the camera. Get the absorption imaging of the MOT.

Note: The atomic number of the MOT is about 10^7 after the pumping phase. A typical absorption image of the MOT is shown in Figure 7a.

6. Preparing an Ultracold Fermi Gas with ODT

6.1. Optical Dipole Trap

Note: ODT is the main tool to generate ultracold Fermi gases. In order to generate a deep ODT, a fiber laser with 100 W emission power at 1064 nm wavelength is used. The setup of ODT is shown in Figure 8.

6.1.1. Turn on the water flow for cooling the laser beam dumps.

6.1.2. Set the ODT AOM control voltage to 1 V manually. Turn on the fiber laser with 13 W emission power.

6.1.3. Check the ODT optics with an infrared light viewer, and remove any dust with argon gas flow.

Note: Dust on the optics can change the spatial profile of the ODT, and cause instability of the ODT.

6.1.4. Command the fiber laser AFG to generate a laser pulse via the AFG control program.

Note: The output of the laser pulse is triggered by the experiment timing, and the starting time of this pulse is set to 14 ms before the end of the MOT loading phase. The pulse sequence control is shown in Figure 1, and the timing is listed in Table 1.

6.1.5. Manually set the ODT AOM control voltage to 8 V (80% of the saturated rf power).

Note: The maximum rf power of the AOM driver should be limited to 80% of the saturated power to reduce the thermal lensing effect.

6.1.6. Acquire the absorption images of the MOT and ODT from the camera.

Note: Check the overlap of the MOT and ODT through their absorption imaging. Figure 7b shows typical absorption images of the MOT and ODT, respectively.

6.2. Bias Magnetic Field and Spin Mixing rf Field

Note: In order to generate an interacting Fermi gas, a bias magnetic field in the vertical direction is applied to tune the *s*-wave scattering length.

6.2.1. Set the H-bridge in the experiment timing program so that the magnetic field configuration changes from anti-Helmholtz to Helmholtz.

Note: The Helmholtz coils generate the bias magnetic field for tuning interatomic interaction.

6.2.2. Set the bias magnetic field to 330 G in channel 2 and 527.3 G in channel 3 of the magnets control program.

6.2.3. Program the experiment timing sequence to sweep the magnetic field from 0 G to 330 G after the MOT is turned off.

Note: This magnetic field sweep prepares a weakly interacting ^{6}Li Fermi gas for standard evaporative cooling.

6.2.4. Program a magnetic field sweep from 330 G to 527 G for a noninteracting Fermi gas[14].

Note: The magnetic field sequence from 6.2.1-6.2.4. is shown in Figure 1, and the timing is listed in Table 1.

6.2.5. Apply a noisy rf pulse to create a 50:50 mixture of the two lowest hyperfine states $2^2S_{1/2}(F = 1/2, m_F = \pm 1/2)$ of ^{6}Li.

6.2.6. Tune the locked laser frequency resonant with the atoms at 527.3 G (corresponding to the transition $2^2S_{1/2}$ $(F = 1/2, m_F = -1/2) \rightarrow 2^2P_{3/2}$ at the low magnetic field) by changing the output frequency of the rf signal generator.

Note: The resonant frequency maximizes the atom number of the absorption imaging, which is used to guide the frequency adjustment. Only the spin-down atoms are imaged to present the atomic cloud because the 50:50 spin mixtures are used for the experiment.

6.3. Evaporative Cooling by Trap Lowering

Note: A standard evaporative cooling is used to cool the fermionic atoms of ^{6}Li near the degenerate regime. The first stage of evaporative cooling is controlled by the pulse of the fiber laser and the second is controlled by the ODT AOM. The near-degenerate Fermi gas will be used as the sample for parametric cooling.

6.3.1. Start the first stage of evaporative cooling with the control software by pulsing the fiber laser power, which increases the trap depth of the ODT to U_0, then back to $0.1U_0$ (U_0 is the full trap depth with the laser power of 100 W). The total time of this stage is 0.5 s.

Note: The pulse duration corresponding to U_0 should be limited to 0.5 s to avoid the thermal lensing effect.

6.3.2. Program the ODT AOM with an exponential curve as shown in Figure 1. After the first stage of evaporative cooling is finished, wait 30 ms, and then start the second stage of evaporative cooling by lowering the trap depth from $0.1U_0$ to $0.01U_0$ through the ODT AOM. The total time of this stage is 1.5 s.

6.3.3. Acquire the absorption imaging of the cold atoms after the evaporative cooling.

Note: About 10^5 atoms are left in the ODT after evaporative cooling, which can be calculated from the absorption image.

7. Parametric Cooling

7.1. Trap Depth Modulation

7.1.1. Wait 100 ms after the magnetic sweep to 527.3 G. Modulate the trap depth with the ODT AOM by $U(t_m) = 0.01U_0(1+\delta\cos(\omega_m t_m))$, where δ is the modulation depth and ω_m is the modulation frequency. Set the modulation time t_m in the parametric modulation AFG control program. The time sequence of the modulation is shown in Figure 1.

Note: This is the key step of implementing parametric cooling.

7.1.2. Program the APG to release the atoms from the ODT by abruptly turning off the trapping beams. Let the gas ballistically expand for 300 µs before applying absorption imaging.

Note: The ballistic expansion is used with TOF absorption imaging to get the temperature of the cold atoms.

7.1.3. Acquire the absorption image of the cold atoms after parametric cooling.

7.2. Time Dependence Measurement

Note: In our previous work[7], we found the optimized frequency of the parametric cooling to be $1.45\omega_x$, where ω_x is the radial trapping frequency of ODT at $0.01U_0$. Using this frequency, we can selectively remove high-energy atoms along the axial direction.

7.2.1. Set the modulation depth to $\delta = 0.5$ via the parametric modulation AFG control program.

7.2.2. Use the external trigger control function of the parametric modulation AFG to change the modulation time from 0 to 600 ms by varying the modulation cycle numbers.

Note: With the increasing of modulation time, the size of the atomic cloud will be reduced, especially the axial direction. The relevant results are shown in Figure 9.

7.2.3. Acquire the imaging frames from the camera. Save and analyze the images through the CCD control program.

REPRESENTATIVE RESULTS:

Using this protocol, we study the dependence of the parametric cooling on the modulation time with the optimized modulation frequency and amplitude, both of which have been determined in our previous publication[7]. We first prepare a noninteracting Fermi gas of ^{6}Li atoms in the two lowest hyperfine states with a temperature of $T/T_F \approx 1.2$. Here, $T_F = (6N)^{1/3}\hbar\omega/k_B = 5.2$ µK is determined with atom number $N = 1.7 \times 10^5$ per spin and the geometric average trapping frequency $\omega = (\omega_x\omega_y\omega_z)^{1/3} = 2\pi \times (2250 \times 2450 \times 220)^{1/3}$ Hz, $\hbar$ is the reduced Planck constant, and k_B is the Boltzmann constant. The time-dependent results are shown in Figure 9 with modulation frequency of $1.45\omega_x$, and modulation depth of 0.5. The TOF absorption images of the atomic clouds (Figure 9a) show a significant decrease of the axial cloud size with the increasing of the modulation time, indicating the absolute temperature is continually reduced by parametric cooling.

For quantitatively describing the cooling effect, we use $E_{(x,z)}/E_F$ as an effective thermometry for ultracold Fermi gases[7], where E_F is the Fermi energy and $E_{(x,z)}$ are the atomic cloud energies in the radial and axial directions respectively. We firstly extract the number independent mean square size (NIMS) from the atomic cloud. Then from the NIMS, we calculate $E_{(x,z)}/E_F$ in Figure 9b. After about 500 ms modulation, the E_z/E_F is reduced significantly from 1.80 to 0.90 and the E_x/E_F is slightly increased slightly from 1.20 to 1.25. The decreasing atomic numbers in Figure 9b inset indicate atoms are expelled out of the trap. We find that parametric cooling changes the atomic cloud energy in an anisotropic way, in which the energy in the axial direction is below the Fermi energy while the radial one is still above the Fermi energy. It is noted that the initial unequal energies in axial and radial direction (Figure 9b) is generated by the fast trap lowering applied in section 6.3. After the parametric cooling, the axial direction energy is significantly reduced while the radial energy is barely changed. This result indicates the way that parametric cooling changes the cloud energy is anisotropic. This anisotropic effect is due to the fact that the dominant anharmonicity of the crossed-beam ODT is along the axial direction[7]. Such thermodynamically anisotropic samples can be used to study thermalization processes in an interacting many-body quantum system.

Figure 1: Ultrahigh vacuum system.

The vacuum chamber of the ultracold atom apparatus at IUPUI. 1. oven, 2. Zeeman slower, 3. magnet coils, 4. experiment chamber and 5. CCD camera.

Figure 2: Timing sequence for the parametric cooling.

The black curve is the fiber laser power timing. The red curve is one of ODT AOM timing. The cyan curve represents the magnetic field. The orange curve is the TOF imaging pulses. The horizontal axis shows the time scale of each stage.

Figure 3: Atomic levels of ^{6}Li and laser frequency locking spectra.
a) ^{6}Li D_2 transition for the cooling and repumping beams of the MOT. **B**) The yellow curve is the Doppler-free saturated absorption spectra of ^{6}Li D_2 line, and the red curve is the related lock-in error signal. The left peak is the $2^2S_{1/2}(F = 3/2) \rightarrow 2^2P_{3/2}$ transition, the right one is the $2^2S_{1/2}(F = 1/2) \rightarrow 2^2P_{3/2}$ transition, and the middle one is the crossover signal of the two transitions. The dash cross is the lock point.

Figure 4: ^{6}Li oven.
Each labeled section contains a temperature controlled heating coil for the oven to output the required atomic flux.

Figure 5: Zeeman slower.
The crossover coil is the last section of the Zeeman slower.

Figure 6: MOT optical layout.
The optical setup for generation of the MOT and slowing laser beams.

Figure 7: MOT and ODT absorption images.
a) MOT image after pumping phase. **b)** The image of the overlapped MOT and ODT.

Figure 8: Crossed-Beam ODT optical layout.
The crossing angle of the ODT is $2\theta = 12°$. The fiber laser AFG controls the pulsing of the laser, the ODT AFG controls the trap lowering curve, and the parametric modulation AFG controls the laser intensity modulation. The beam waist of both beams is about 37 µm. The polarization of the first beam is vertical and the polarization of the second beam is horizontal.

Figure 9: Time dependence measurement of parametric cooling.
a) The absorption images of the atomic clouds of various modulation times. **b**) The dependence of $E_{(x,z)}/E_F$ on modulation time (blue circles are for E_z/E_F and the red squares are for E_x/E_F). The inset figure is the atom number versus modulation time. Error bars represent one standard deviation.

Table 1: Experimental timing control.
Timing sequence parameters to control experimental instruments. The timing sequence starts at MOT loading, cooling and pumping. The MOT off is the time point of after MOT pumping.

Table 2: Oven temperature profile.
The ^{6}Li oven operates at optimal flux with the listed temperatures.

Table 3: MOT phases properties.
The MOT phase sequence is designed to maximize the number of atoms to be transferred into the ODT.

DISCUSSION:

We present an experimental protocol for parametric cooling of a noninteracting Fermi gas in a crossed-beam optical trap. The critical steps of this protocol include: First, the optically-trapped Fermi gas needs to be cooled close to the degenerate temperature by lowering the trap depth. Second, a modulation frequency is chosen that is resonant with the anharmonic component of the trapping potential. Third, the intensity of the trapping beam is modulated to cool the atomic cloud and measure the dependence of the cloud energy on the modulation time.

Compared with the trap-lowering scheme, the parametric cooling scheme provides a selective way to remove high-energy atoms from the optical trap without lowering the trap depth. It helps to increase the phase density and cool a noninteracting Fermi gas. Because such parametric cooling is usually anisotropic, it also provides a convenient method to modify temperature anisotropy in quantum gases.

To enable parametric cooling, the current protocol requires a Fermi gas near the degenerate temperature as the starting point. The cooling effect is also limited to the axial direction of the trapping potential. These two limitations are caused by the finite anharmonicity of the crossed-beam ODT that is made by Gaussian laser beams in the current protocol. To extend this method for different atomic species and apply it for larger temperature range, we need to increase the anharmonicity of the trapping potential.

We propose two improvements for this cooling technique. First, parametric cooling can be implemented with a trapping potential with large anharmonicity in all three directions, such as box traps[15] or power-law traps[16], which has the potential to directly cool the trapped atoms from the thermal state into the degenerate regime without requiring lowering the optical trap at all. Second, by periodically shaking the optical trapping potential through an AOM[17], we can synthesize the optical trap with large anharmonicity using the Floquet method[18].

ACKNOWLEDGMENTS:
We thank Ji Liu and Wen Xu for involving in the experimental setup. Le Luo is a member of the Indiana University Center for Spacetime Symmetries (IUCSS). This work was supported by IUPUI and IUCRG.

DISCLOSURES:
The authors have nothing to disclose. Specific product and company citations are for the purpose of clarification only and are not an endorsement by the authors.

REFERENCES:
1. Petrich, W., Anderson, M. H., Ensher, J. R. & Cornell, E. A. Stable, tightly confining magnetic trap for evaporative cooling of neutral atoms. *Phys. Rev. Lett.* **74** (17), 3352, doi: 10.1103/PhysRevLett.74.3352 (1995).
2. Ketterle, W. & Druten, N. J. V. Evaporative cooling of trapped atoms. In: *Advances in Atomic, Molecular, and Optical Physics*. **37**, Bederson, B. & Walther, H. eds., 181-236, doi: 10.1016/S1049-250X(08)60101-9 Academic Press (2003).

3. Truscott, A. G., Strecker, K. E., McAlexander, W. I., Partridge, G. B. & Hulet, R. G. Observation of Fermi pressure in a gas of trapped atoms. *Science.* **291** (5513), 2570-2572, doi: 10.1126/science.1059318 (2001).
4. DeMarco, B. & Jin, D. S. Onset of Fermi degeneracy in a trapped atomic gas. *Science.* **285** (5434), 1703-1706, doi: 10.1126/science.285.5434.1703 (1999).
5. S. R. Granade, M. E. Gehm, K. M. O'Hara, & J. E. Thomas. All-optical production of a degenerate Fermi gas. *Phys. Rev. Lett.* **88** (12), 120405, doi: 10.1103/PhysRevLett.88.120405 (2002).
6. Luo, L., *et al.* Evaporative cooling of unitary Fermi gas mixtures in optical traps. *New J. Phys.* **8** (9), 213, doi: 10.1088/1367-2630/8/9/213 (2006).
7. Li, J., Liu, J., Xu, W., de Melo, L. & Luo, L. Parametric cooling of a degenerate Fermi gas in an optical trap. *Phys. Rev. A*. **93** (4), 041401, doi: 10.1103/PhysRevA.93.041401 (2016).
8. Poli, N., Brecha, R. J., Roati, G. & Modugno, G. Cooling atoms in an optical trap by selective parametric excitation. *Phys. Rev. A.* **65** (2), 021401, doi: 10.1103/PhysRevA.65.021401 (2002).
9. Kumakura, M., Shirahata, Y., Takasu, Y., Takahashi, Y. & Yabuzaki, T. Shaking-induced cooling of cold atoms in a magnetic trap. *Phys. Rev. A.* **68** (2), 021401, doi: 10.1103/PhysRevA.68.021401 (2003).
10. Li, J., *et al.* Sub-megahertz frequency stabilization of a diode laser by digital laser current modulation. *Appl. Opt.* **54** (13), 3913-3917, doi: 10.1364/AO.54.003913 (2015).
11. *HiPic user manual*. Hamamatsu Photonics Deutschland GmbH (2016).
12. Luo, L. *Entropy and superfluid critical parameters of a strongly interacting Fermi gas*. Ph.D. thesis, Duke University (2008).
13. Ries, M. *A magneto-optical trap for the preparation of a three-component Fermi gas in an optical lattice*. Diploma thesis, University of Heidelberg (2010).
14. Bartenstein, M., *et al*. Precise determination of ^{6}Li cold collision parameters by radio-frequency spectroscopy on weakly bound molecules. *Phys. Rev. Lett*. **94** (10), 103201, doi: 10.1103/PhysRevLett.94.103201 (2005).
15. Gaunt, A. L., Schmidutz, T. F., Gotlibovych, I., Smith, R. P. & Hadzibabic, Z. Bose-Einstein condensation of atoms in a uniform potential. *Phys. Rev. Lett*. **110** (20), 200406, doi: 10.1103/PhysRevLett.110.200406 (2013).
16. Bruce, G. D., Bromley, S. L., Smirne, G., Torralbo-Campo, L. & Cassettari, D. Holographic power-law traps for the efficient production of Bose-Einstein condensates. *Phys. Rev. A*. **84** (5), 053410, doi: 10.1103/PhysRevA.84.053410 (2011).
17. Roy, R., Green, A., Bowler, R. & Gupta, S. Rapid cooling to quantum degeneracy in dynamically shaped atom traps. *Phys. Rev. A*. **93** (4), 043403, doi: 10.1103/PhysRevA.93.043403 (2016).
18. Bukov, M., D’Alessio, L. & Polkovnikov, A. Universal high-frequency behavior of periodically driven systems: from dynamical stabilization to Floquet engineering. *Adv. Phys.* **64** (2), 139-226, doi: 10.1080/00018732.2015.1055918 (2015).

Figure

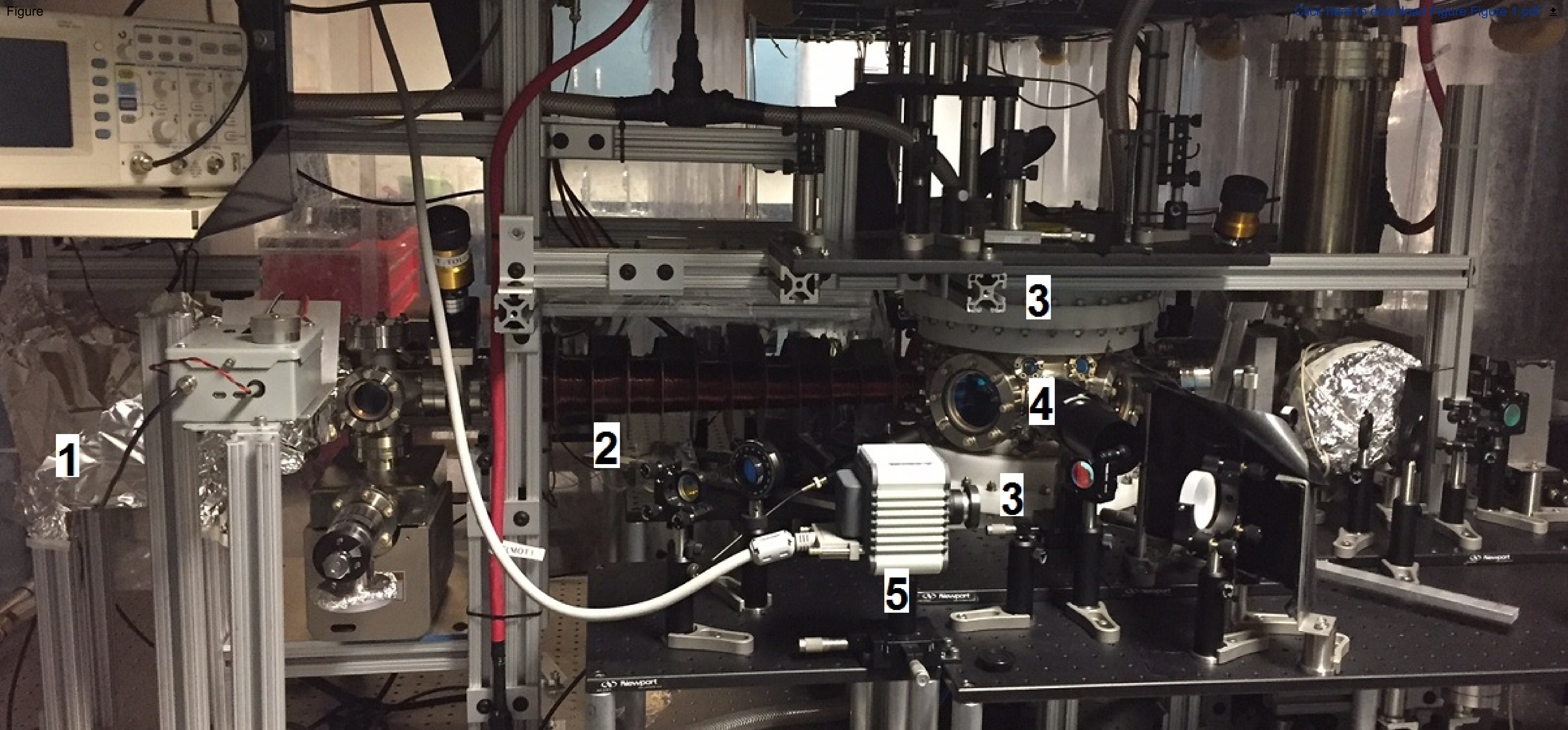

Figure

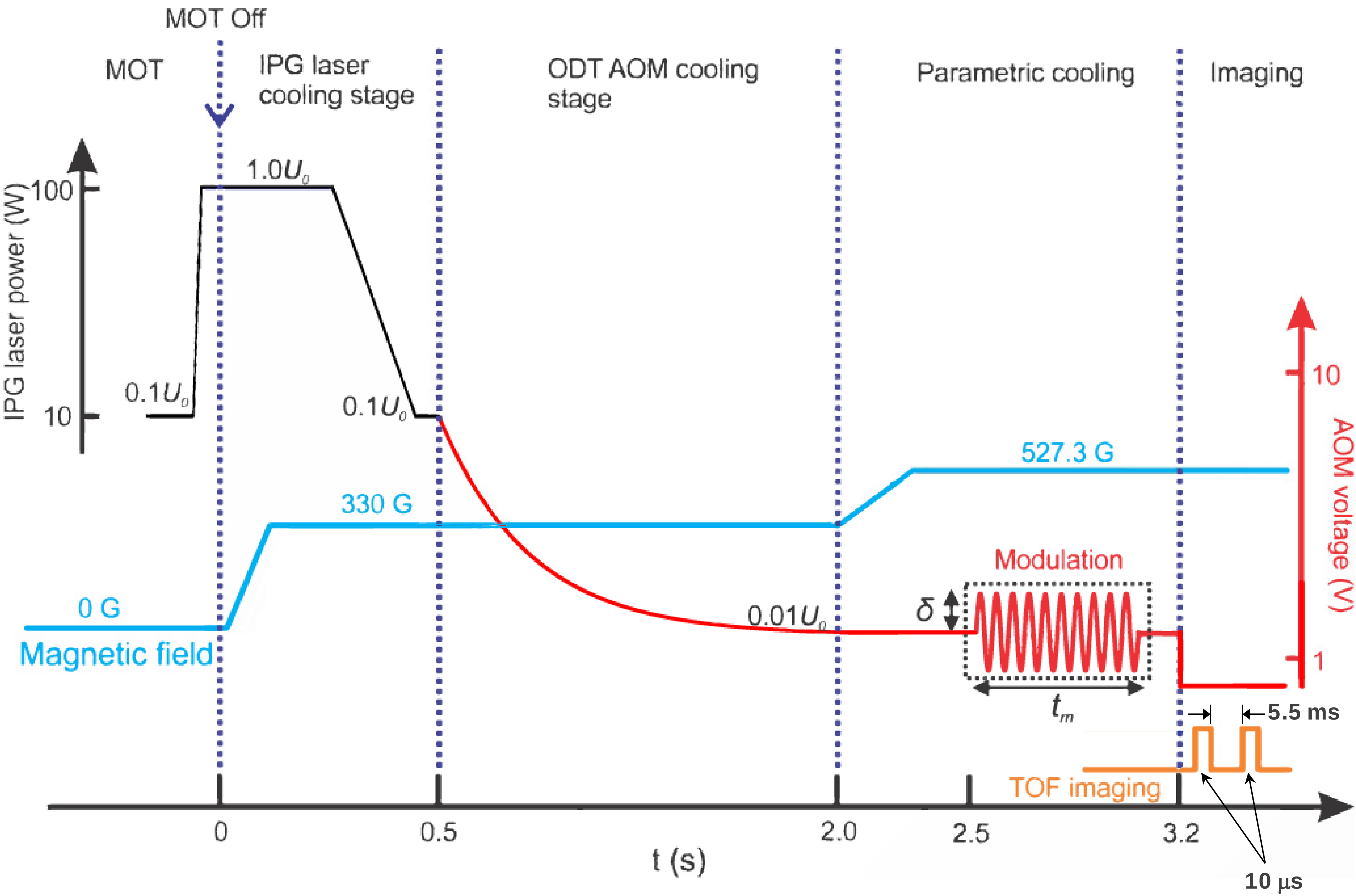
MOT Off
MOT
IPG laser cooling stage
ODT AOM cooling stage
Parametric cooling
Imaging
IPG laser power (W)
100
10
1.0U_0
0.1U_0
0.1U_0
0.01U_0
330 G
527.3 G
0 G
Magnetic field
Modulation
δ
t_m
AOM voltage (V)
10
1
5.5 ms
TOF imaging
10 μs
0
0.5
2.0
2.5
3.2
t (s)

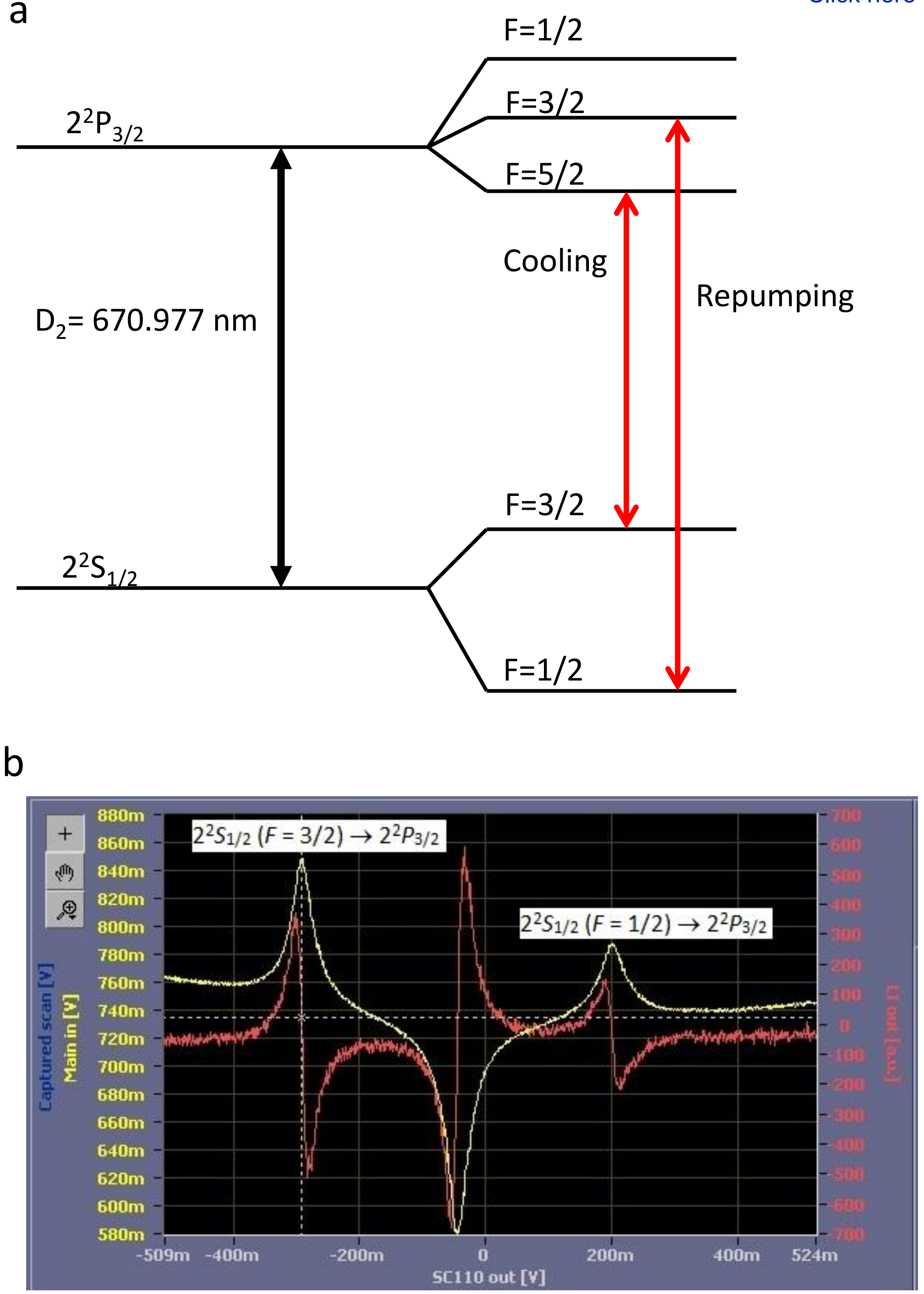
a
F=1/2
F=3/2
F=5/2
2²P3/2
D2= 670.977 nm
Cooling
Repumping
F=3/2
2²S1/2
F=1/2
b
2²S1/2 (F = 3/2) → 2²P3/2
2²S1/2 (F = 1/2) → 2²P3/2
Captured scan [V]
Main in [V]
Et out [au]
SC110 out [V]
880m
860m
840m
820m
800m
780m
760m
740m
720m
700m
680m
660m
640m
620m
600m
580m
-509m
-400m
-200m
0
200m
400m
524m
700
600
500
400
300
200
100
0
-100
-200
-300
-400
-500
-600
-700

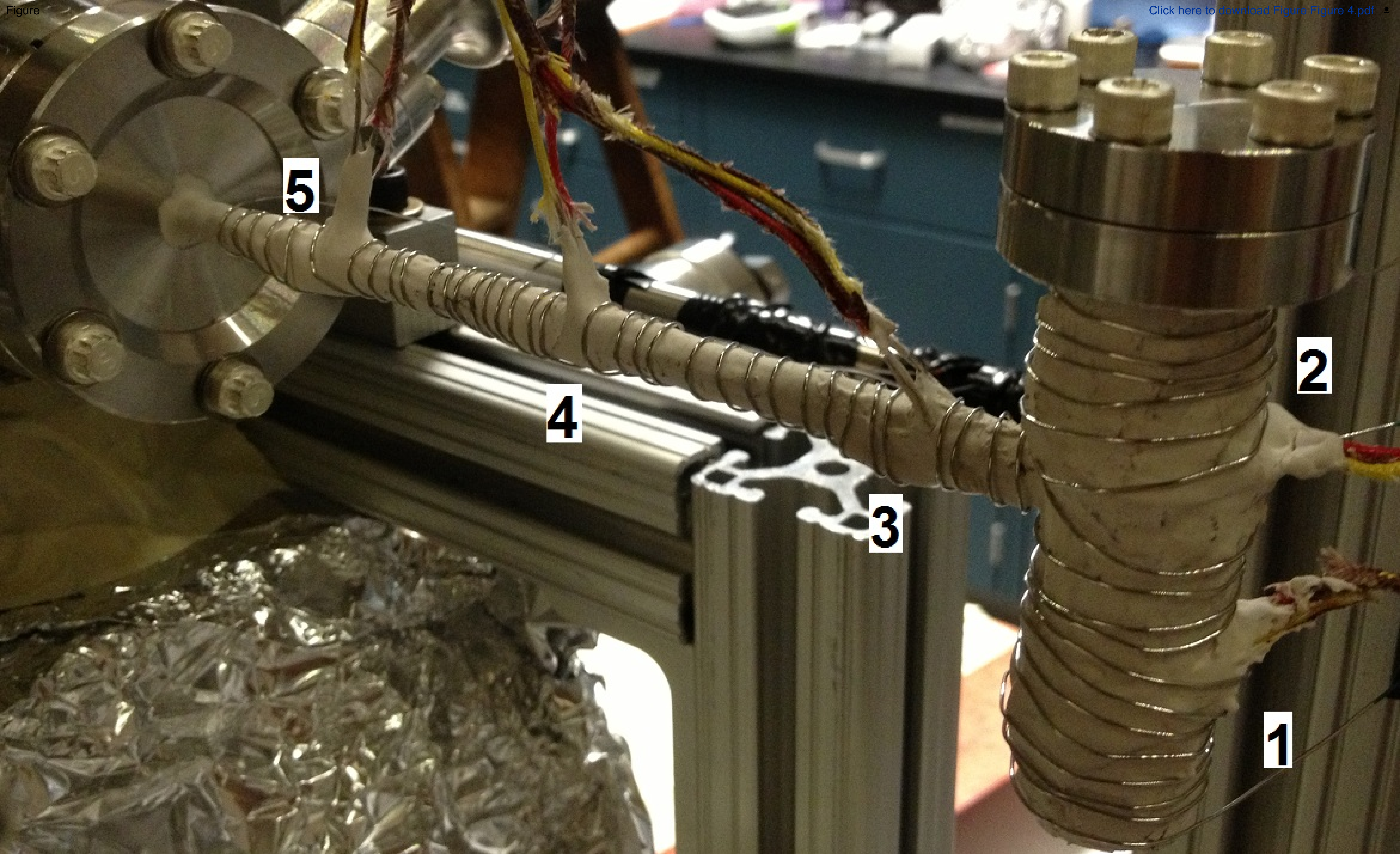
5
4
3
2
1

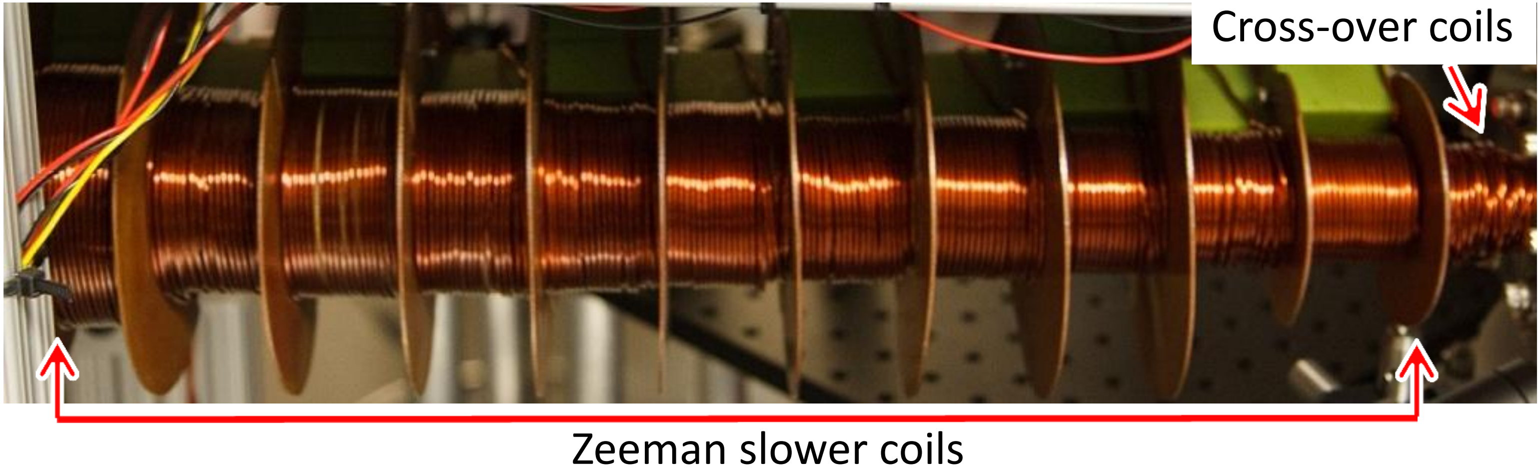
Cross-over coils
Zeeman slower coils

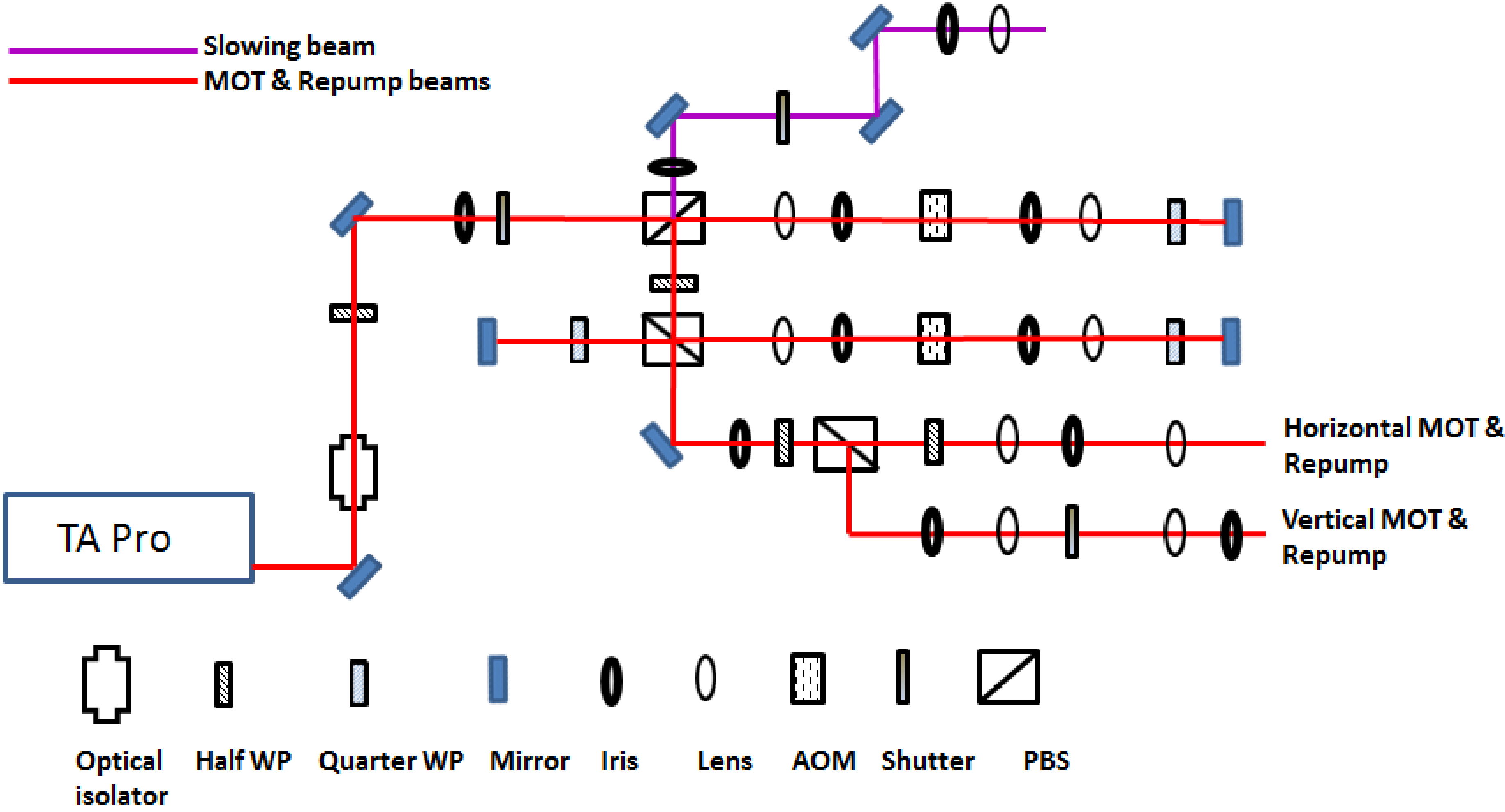
Slowing beam
MOT & Repump beams
TA Pro
Horizontal MOT &
Repump
Vertical MOT &
Repump
Optical isolator
Half WP
Quarter WP
Mirror
Iris
Lens
AOM
Shutter
PBS

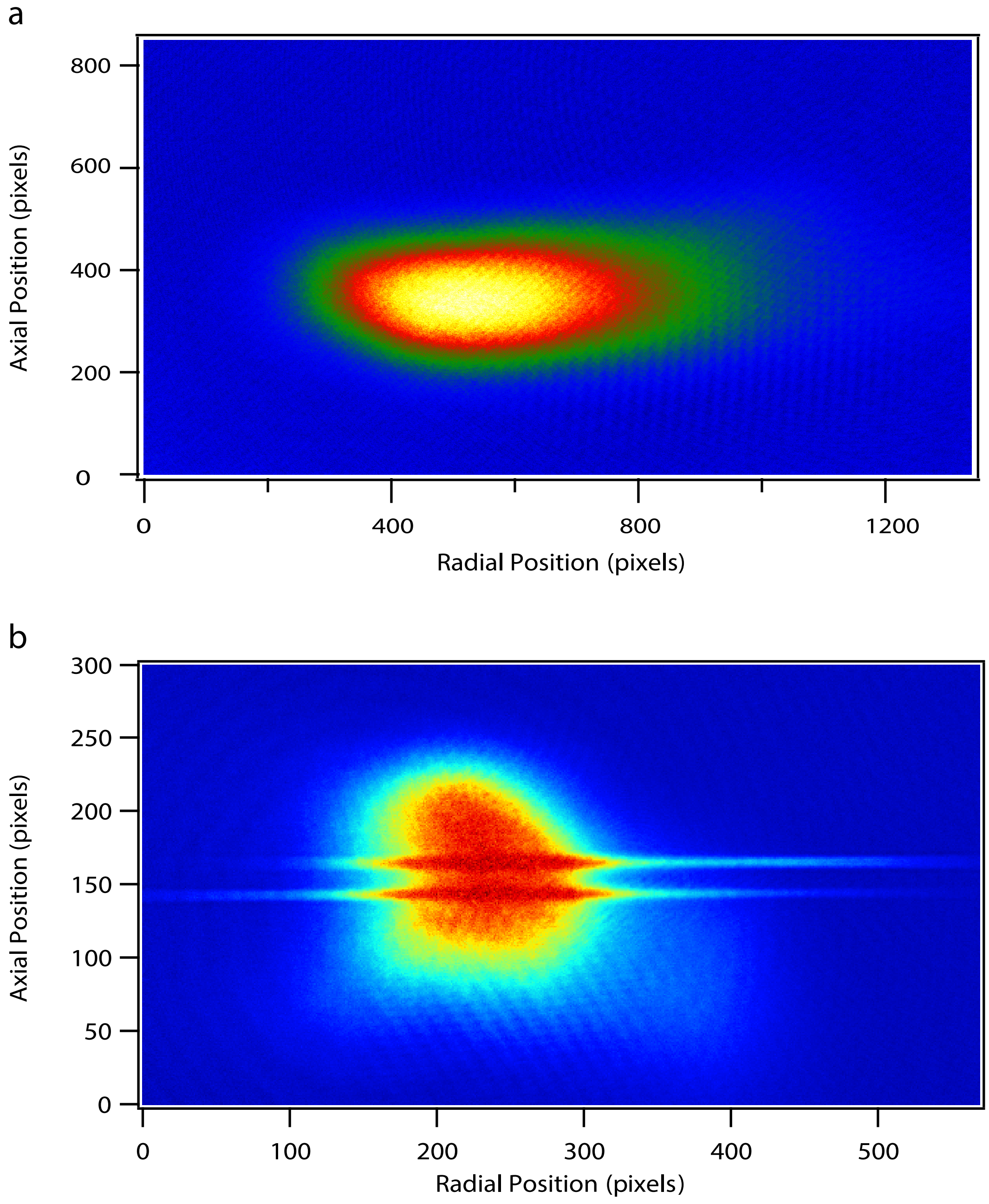
a
800
600
400
200
0
Axial Position (pixels)
0
400
800
1200
Radial Position (pixels)
b
300
250
200
150
100
50
0
Axial Position (pixels)
0
100
200
300
400
500
Radial Position (pixels)

Figure

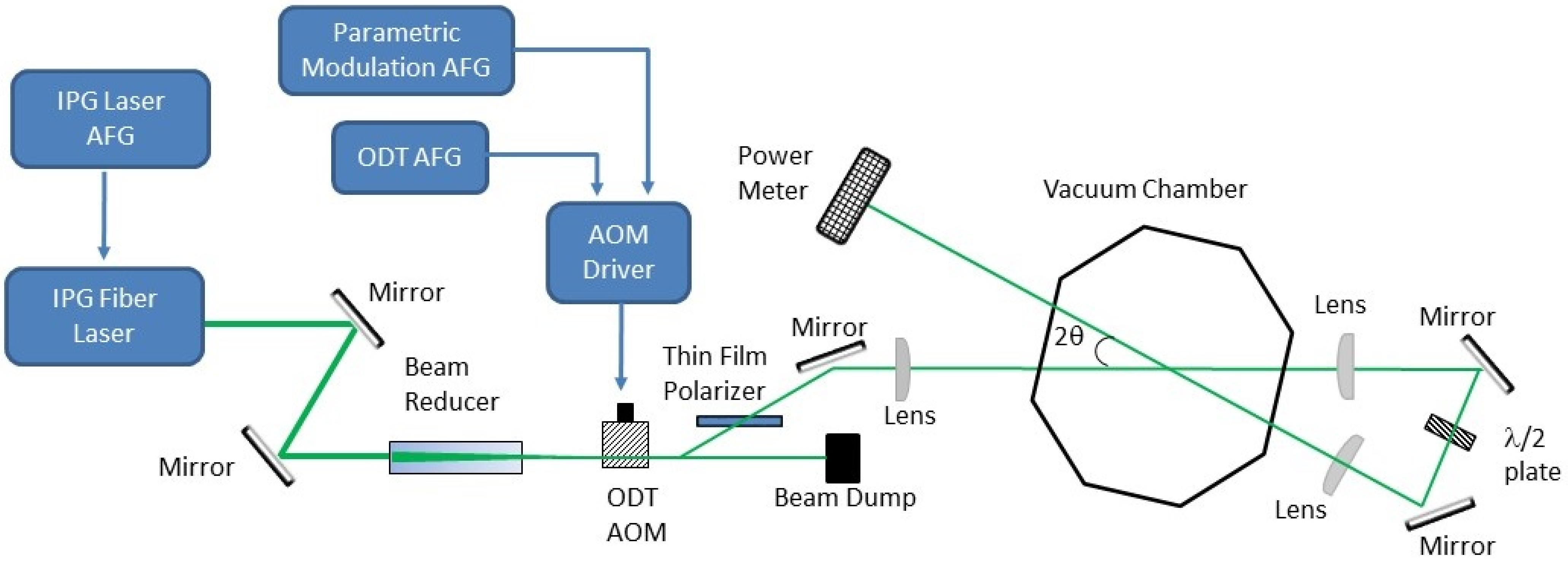
Parametric Modulation AFG
IPG Laser AFG
ODT AFG
AOM Driver
IPG Fiber Laser
Mirror
Beam Reducer
Mirror
ODT AOM
Thin Film Polarizer
Mirror
Lens
Beam Dump
Power Meter
Vacuum Chamber
2θ
Lens
Mirror
λ/2 plate
Lens
Mirror

Figure
Click here to download Figure Figure 9.pdf

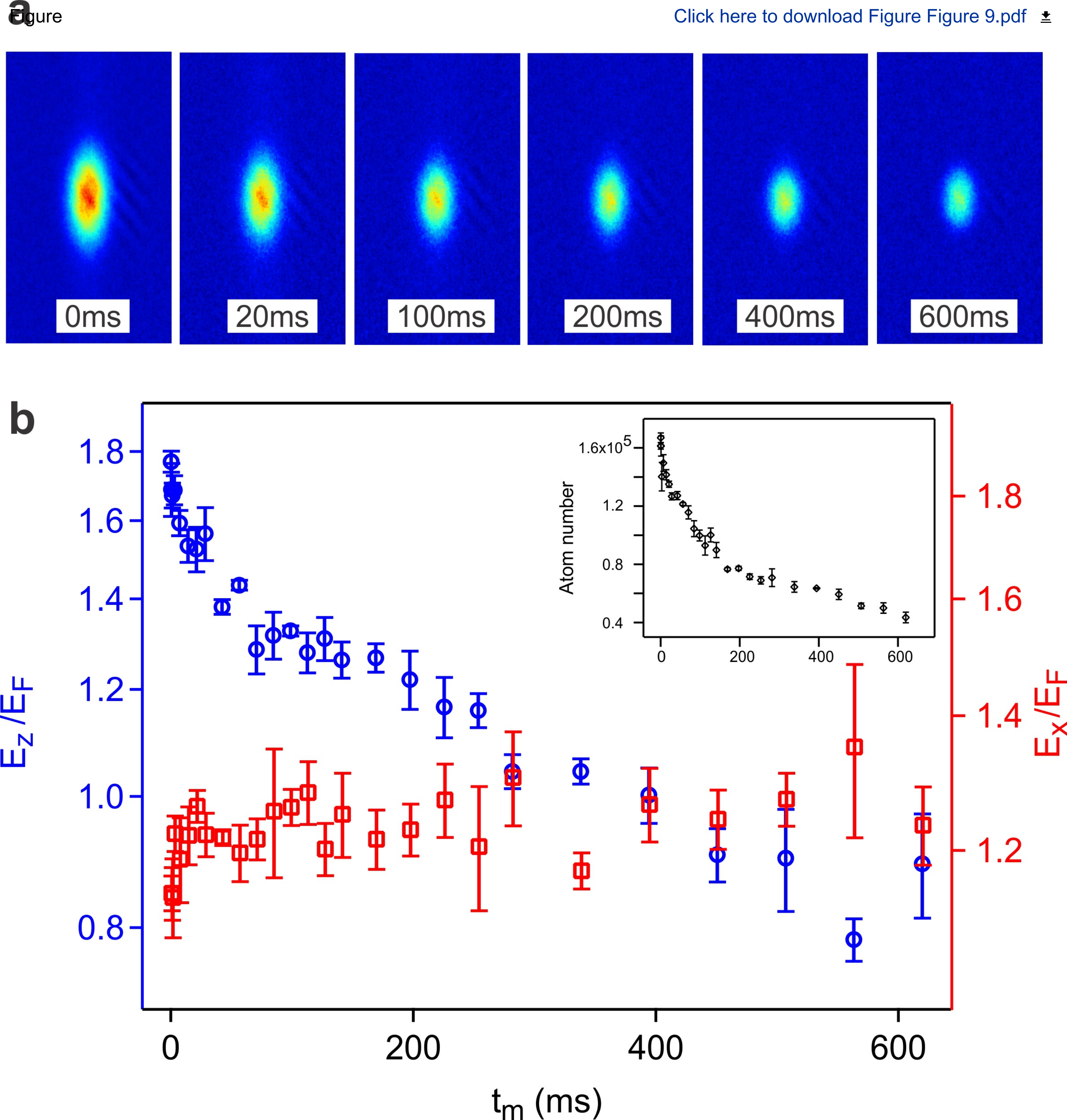

Table

Click here to download Table Table 1.xlsx

MOT loading on	Start point
MOT loading time	10 s
MOT cooling on	MOT loading off
MOT cooling time	5 ms
MOT pumping on	MOT cooling off
MOT pumping time	100 µs
MOT AOM off	MOT off (The same as MOT pumping off)
Zeeman slower beam shutter on	200 ms before the MOT loading off
MOT beam shutter on	MOT off
Fiber laser evaporative cooling start time	14 ms before the end of MOT loading
ODT evaporative cooling start time	500 ms after MOT off
H-bridge switch time	MOT off
Magnetic field sweep start time (from 0 to 330 G)	MOT off
Magnetic field sweep start time (from 330 to 527.3G)	2000 ms after MOT off
Parametric cooling start time	2500 ms after MOT off
Imaging pluse trigger time	3200 ms after MOT off
CCD trigger time	100 µs before the imaging pluse trigger time

Table

Click here to download Table Table 2.xlsx

Channel 1	Channel 2	Channel 3	Channel 4	Channel 5
348 °C	354 °C	434 °C	399 °C	372 °C

Table

Click here to download Table Table 3.xlsx

Phase	Loading		Cooling		Pumping	
Beam	Cooling	Repumping	Cooling	Repumping	Cooling	Repumping
Detuning from locked transition(MHz)	-28	-28	-5	-5	-2	OFF
Intensity (I_{sat})	2	1	0.1	0.05	0.08	OFF

Name	Company	Catalog Number	Comments/Description
500 mW 671 nm ECDL	Toptica	TA Pro	Quantity:1
35 mW 671 nm ECDL	Toptica	DL-100	Quantity:1
671 nm AOM	Isomet	1206C	Quantity:3
671 nm AOM Driver	Isomet	630C-110	Quantity:3
100 W 1064 nm CW laser	IPG photonics	YLR-100-1064-LP	Quantity:1
1064 nm AOM	IntraAction	ATM-804DA6B	Quantity:1
1064 nm AOM Driver	IntraAction	ME-805EH	Quantity:1
Arbitrary Function Generator	Agilent	33120A	Quantity:3
Digital I/O Board	United Electronic Industries	PD2-DIO-128	Quantity:1
System Design Platform	National Instruments	LabVIEW	Quantity:1
Analog Voltage Output Device	Measurement Computing	USB-3104	Quantity:1
CCD Camera	Hamamatsu	Orca R2	Quantity:1
Arbitrary Pulse Generator	Quantum Composer	9618+	Quantity:1
Analog Voltage Output Device	Measurement Computing	USB-3104	Quantity:1
20 A power supply			Quantity:1
10 A power supply			Quantity:1
120 A power supply			Quantity:2
Cooling Fans			Quantity: depends on apparatus design
671 nm Mirrors			Quantity: depends on apparatus design
671 nm Half-wave Plate			Quantity: depends on apparatus design
671 nm Quarter-wave Plate			Quantity: depends on apparatus design
500 mW Beam Shutter			Quantity: depends on apparatus design
671 nm Lenses			Quantity: depends on apparatus design
Faraday Isolator			Quantity: 2, one for each ECDL
671 nm Polarizing Beam Splitter			Quantity: depends on apparatus design
Photodetector	Thorlabs	SM05PD1A	Quantity:1
Multiplexer	Analog Devices	ADG409	Quantity: 1
Multiplexer	Analog Devices	ADG408	Quantity: 2
1064 nm plano-concave lens			Quantity:1 for beam reducer
1064 nm plano-convex lens			Quantity:1 for beam reducer
1064 nm Mirrors			Quantity: depends on apparatus design
1064 nm Half-wave Plates			Quantity: depends on apparatus design
1064 nm Lenses			Quantity: depends on apparatus design
1064 nm Thin Film Polarizer			Quantity:1
100 W, 1064 nm Beam Dump			Quantity:1
100 W, 1064 nm Power Meter			Quantity:1
RF Function Generator	Rigol	DG4162	Quantity:1
RF Power Amplifier	Mini-Circuits	ZHL-100W-GAN+	Quantity:1

JoVE JOURNAL OF VISUALIZED EXPERIMENTS
1 Alewife Center #200
Cambridge, MA 02140
tel. 617.945.9051
www.jove.com

ARTICLE AND VIDEO LICENSE AGREEMENT

Title of Article: Cooling an optically-trapped ultracold Fermi gas by periodical driving

Author(s): Jiaming Li, Leonardo Fonseca de Melo, Le Luo

Item 1 (check one box): The Author elects to have the Materials be made available (as described at http://www.jove.com/publish) via: ☒ Standard Access ☐ Open Access

Item 2 (check one box):

☒ The Author is NOT a United States government employee.

☐ The Author is a United States government employee and the Materials were prepared in the course of his or her duties as a United States government employee.

☐ The Author is a United States government employee but the Materials were NOT prepared in the course of his or her duties as a United States government employee.

ARTICLE AND VIDEO LICENSE AGREEMENT

1. Defined Terms. As used in this Article and Video License Agreement, the following terms shall have the following meanings: "**Agreement**" means this Article and Video License Agreement; "**Article**" means the article specified on the last page of this Agreement, including any associated materials such as texts, figures, tables, artwork, abstracts, or summaries contained therein; "**Author**" means the author who is a signatory to this Agreement; "**Collective Work**" means a work, such as a periodical issue, anthology or encyclopedia, in which the Materials in their entirety in unmodified form, along with a number of other contributions, constituting separate and independent works in themselves, are assembled into a collective whole; "**CRC License**" means the Creative Commons Attribution-Non Commercial-No Derivs 3.0 Unported Agreement, the terms and conditions of which can be found at: http://creativecommons.org/licenses/by-nc-nd/3.0/legalcode; "**Derivative Work**" means a work based upon the Materials or upon the Materials and other pre-existing works, such as a translation, musical arrangement, dramatization, fictionalization, motion picture version, sound recording, art reproduction, abridgment, condensation, or any other form in which the Materials may be recast, transformed, or adapted; "**Institution**" means the institution, listed on the last page of this Agreement, by which the Author was employed at the time of the creation of the Materials; "**JoVE**" means MyJove Corporation, a Massachusetts corporation and the publisher of *The Journal of Visualized Experiments;* "**Materials**" means the Article and / or the Video; "**Parties**" means the Author and JoVE; "**Video**" means any video(s) made by the Author, alone or in conjunction with any other parties, or by JoVE or its affiliates or agents, individually or in collaboration with the Author or any other parties, incorporating all or any portion of the Article, and in which the Author may or may not appear.

2. Background. The Author, who is the author of the Article, in order to ensure the dissemination and protection of the Article, desires to have the JoVE publish the Article and create and transmit videos based on the Article. In furtherance of such goals, the Parties desire to memorialize in this Agreement the respective rights of each Party in and to the Article and the Video.

3. Grant of Rights in Article. In consideration of JoVE agreeing to publish the Article, the Author hereby grants to JoVE, subject to **Sections 4** and **7** below, the exclusive, royalty-free, perpetual (for the full term of copyright in the Article, including any extensions thereto) license (a) to publish, reproduce, distribute, display and store the Article in all forms, formats and media whether now known or hereafter developed (including without limitation in print, digital and electronic form) throughout the world, (b) to translate the Article into other languages, create adaptations, summaries or extracts of the Article or other Derivative Works (including, without limitation, the Video) or Collective Works based on all or any portion of the Article and exercise all of the rights set forth in (a) above in such translations, adaptations, summaries, extracts, Derivative Works or Collective Works and (c) to license others to do any or all of the above. The foregoing rights may be exercised in all media and formats, whether now known or hereafter devised, and include the right to make such modifications as are technically necessary to exercise the rights in other media and formats. If the "Open Access" box has been checked in **Item 1** above, JoVE and the Author hereby grant to the public all such rights in the Article as provided in, but subject to all limitations and requirements set forth in, the CRC License.

4. Retention of Rights in Article. Notwithstanding the exclusive license granted to JoVE in **Section 3** above, the Author shall, with respect to the Article, retain the non-exclusive right to use all or part of the Article for the non-commercial purpose of giving lectures, presentations or teaching classes, and to post a copy of the Article on the Institution's website or the Author's personal website, in each case provided that a link to the Article on the JoVE website is provided and notice of JoVE's copyright in the Article is included. All non-copyright intellectual property rights in and to the Article, such as patent rights, shall remain with the Author.

5. Grant of Rights in Video – Standard Access. This **Section 5** applies if the "Standard Access" box has been checked in **Item 1** above or if no box has been checked in **Item 1** above. In consideration of JoVE agreeing to produce, display or otherwise assist with the Video, the Author hereby acknowledges and agrees that, Subject to **Section 7** below, JoVE is and shall be the sole and exclusive owner of all rights of any nature, including, without limitation, all copyrights, in and to the Video. To the extent that, by law, the Author is deemed, now or at any time in the future, to have any rights of any nature in or to the Video, the Author hereby disclaims all such rights and transfers all such rights to JoVE.

6. Grant of Rights in Video – Open Access. This **Section 6** applies only if the "Open Access" box has been checked in **Item 1** above. In consideration of JoVE agreeing to produce, display or otherwise assist with the Video, the Author hereby grants to JoVE, subject to **Section 7** below, the exclusive, royalty-free, perpetual (for the full term of copyright in the Article, including any extensions thereto) license (a) to publish, reproduce, distribute, display and store the Video in all forms, formats and media whether now known or hereafter developed (including without limitation in print, digital and electronic form) throughout the world, (b) to translate the Video into other languages, create adaptations, summaries or extracts of the Video or other Derivative Works or Collective Works based on all or any portion of the Video and exercise all of the rights set forth in (a) above in such translations, adaptations, summaries, extracts, Derivative Works or Collective Works and (c) to license others to do any or all of the above. The foregoing rights may be exercised in all media and formats, whether now known or hereafter devised, and include the right to make such modifications as are technically necessary to exercise the rights in other media and formats. For any Video to which this Section 6 is applicable, JoVE and the Author hereby grant to the public all such rights in the Video as provided in, but subject to all limitations and requirements set forth in, the CRC License.

7. Government Employees. If the Author is a United States government employee and the Article was prepared in the course of his or her duties as a United States government employee, as indicated in **Item 2** above, and any of the licenses or grants granted by the Author hereunder exceed the scope of the 17 U.S.C. 403, then the rights granted hereunder shall be limited to the maximum rights permitted under such statute. In such case, all provisions contained herein that are not in conflict with such statute shall remain in full force and effect, and all provisions contained herein that do so conflict shall be deemed to be amended so as to provide to JoVE the maximum rights permissible within such statute.

8. Likeness, Privacy, Personality. The Author hereby grants JoVE the right to use the Author's name, voice, likeness, picture, photograph, image, biography and performance in any way, commercial or otherwise, in connection with the Materials and the sale, promotion and distribution thereof. The Author hereby waives any and all rights he or she may have, relating to his or her appearance in the Video or otherwise relating to the Materials, under all applicable privacy, likeness, personality or similar laws.

9. Author Warranties. The Author represents and warrants that the Article is original, that it has not been published, that the copyright interest is owned by the Author (or, if more than one author is listed at the beginning of this Agreement, by such authors collectively) and has not been assigned, licensed, or otherwise transferred to any other party. The Author represents and warrants that the author(s) listed at the top of this Agreement are the only authors of the Materials. If more than one author is listed at the top of this Agreement and if any such author has not entered into a separate Article and Video License Agreement with JoVE relating to the Materials, the Author represents and warrants that the Author has been authorized by each of the other such authors to execute this Agreement on his or her behalf and to bind him or her with respect to the terms of this Agreement as if each of them had been a party hereto as an Author. The Author warrants that the use, reproduction, distribution, public or private performance or display, and/or modification of all or any portion of the Materials does not and will not violate, infringe and/or misappropriate the patent, trademark, intellectual property or other rights of any third party. The Author represents and warrants that it has and will continue to comply with all government, institutional and other regulations, including, without limitation all institutional, laboratory, hospital, ethical, human and animal treatment, privacy, and all other rules, regulations, laws, procedures or guidelines, applicable to the Materials, and that all research involving human and animal subjects has been approved by the Author's relevant institutional review board.

10. JoVE Discretion. If the Author requests the assistance of JoVE in producing the Video in the Author's facility, the Author shall ensure that the presence of JoVE employees, agents or independent contractors is in accordance with the relevant regulations of the Author's institution. If more than one author is listed at the beginning of this Agreement, JoVE may, in its sole discretion, elect not take any action with respect to the Article until such time as it has received complete, executed Article and Video License Agreements from each such author. JoVE reserves the right, in its absolute and sole discretion and without giving any reason therefore, to accept or decline any work submitted to JoVE. JoVE and its employees, agents and independent contractors shall have

full, unfettered access to the facilities of the Author or of the Author's institution as necessary to make the Video, whether actually published or not. JoVE has sole discretion as to the method of making and publishing the Materials, including, without limitation, to all decisions regarding editing, lighting, filming, timing of publication, if any, length, quality, content and the like.

11. Indemnification. The Author agrees to indemnify JoVE and/or its successors and assigns from and against any and all claims, costs, and expenses, including attorney's fees, arising out of any breach of any warranty or other representations contained herein. The Author further agrees to indemnify and hold harmless JoVE from and against any and all claims, costs, and expenses, including attorney's fees, resulting from the breach by the Author of any representation or warranty contained herein or from allegations or instances of violation of intellectual property rights, damage to the Author's or the Author's institution's facilities, fraud, libel, defamation, research, equipment, experiments, property damage, personal injury, violations of institutional, laboratory, hospital, ethical, human and animal treatment, privacy or other rules, regulations, laws, procedures or guidelines, liabilities and other losses or damages related in any way to the submission of work to JoVE, making of videos by JoVE, or publication in *JoVE* or elsewhere by JoVE. The Author shall be responsible for, and shall hold JoVE harmless from, damages caused by lack of sterilization, lack of cleanliness or by contamination due to the making of a video by JoVE its employees, agents or independent contractors. All sterilization, cleanliness or decontamination procedures shall be solely the responsibility of the Author and shall be undertaken at the Author's expense. All indemnifications provided herein shall include JoVE's attorney's fees and costs related to said losses or damages. Such indemnification and holding harmless shall include such losses or damages incurred by, or in connection with, acts or omissions of JoVE, its employees, agents or independent contractors.

12. Fees. To cover the cost incurred for publication, JoVE must receive payment before production and publication the Materials. Payment is due in 21 days of invoice. Should the Materials not be published due to an editorial or production decision, these funds will be returned to the Author. Withdrawal by the Author of any submitted Materials after final peer review approval will result in a US$1,200 fee to cover pre-production expenses incurred by JoVE. If payment is not received by the completion of filming, production and publication of the Materials will be suspended until payment is received.

13. Transfer, Governing Law. This Agreement may be assigned by JoVE and shall inure to the benefits of any of JoVE's successors and assignees. This Agreement shall be governed and construed by the internal laws of the Commonwealth of Massachusetts without giving effect to any conflict of law provision thereunder. This Agreement may be executed in counterparts, each of which shall be deemed an original, but all of which together shall be deemed to me one and the same agreement. A signed copy of this Agreement delivered by facsimile, e-mail or other means of electronic transmission shall be deemed to have the same legal effect as delivery of an original signed copy of this Agreement.

A signed copy of this document must be sent with all new submissions. Only one Agreement required per submission.

CORRESPONDING AUTHOR:

Name: Le Luo

Department: Physics

Institution: Indiana University Purdue University Indianapolis

Article Title: Cooling an optically-trapped ultracold Fermi gas by periodical driving

Signature: Le Luo Date: 8-29-2016

Please submit a signed and dated copy of this license by one of the following three methods:

1) Upload a scanned copy of the document as a pfd on the JoVE submission site;
2) Fax the document to +1.866.381.2236;
3) Mail the document to JoVE / Attn: JoVE Editorial / 1 Alewife Center #200 / Cambridge, MA 02139

For questions, please email submissions@jove.com or call +1.617.945.9051

Dr. Nam Nguyen
Editor, Journal of Visualized Experiments

Dear Dr. Nguyen,

We would appreciate the opportunity to resubmit our paper, "Cooling an optically-trapped ultracold Fermi gas by periodical driving", in response to the editorial comments and comments from reviewer #1, which have been addressed individually as follows.

Editorial comments:
1.Additional detail is required in numerous steps:

"If locking a laser is a multistep process, please provide a citation for the method used."
Response: Locking the ECDL frequency is indeed a multistep process, so in Section 3 Note. We have included "A digital laser current modulation method (DLCM) is applied for laser frequency stabilization[10]". Ref 10 is our previous publication *Appl. Opt.* 54 (13), 3913-3917, which provides the details of locking procedure.

"Is the camera used at earlier steps in the protocol? It would be better to incorporate instructions for use of the camera when it is first used. We won't film this separately as written."
Response: The camera is used in an earlier step in the protocol. We accepted the editor's suggestion to move the camera section to section 2 so that camera usage instructions are described before any steps that require the camera.

2. Formatting: Make sure that narrative descriptions of what is happening occur as notes and are not included with the action in the step.
Response: We have removed the narrative descriptions and have kept the narrative as notes so that they contain important information about what to expect from the steps.

3. Visualization: Make sure to provide labeled, photographic images of the setup/equipment. These can be provided as supplemental files.
Response: we provide labeled photographic images of the equipment in the supplemental files, including 1. apparatus, 2.laser locking, 3.mot optics, 4.Fiber laser, 5. Offset locking.

Reviewers' comments:

Reviewer #1:
The reviewer #1 suggested us to provide more details so that the reader can follow the experimental procedure. We accepted the reviewer's suggestion and made the following improvements.

1."the current of the slower and crossover coils in section 2.2.2 and the photodetector voltage in 2.4.1 were given, but the coil design and the MOT fluorescence intensity were not explained."
Response: The Zeeman slower coil is shown in Figure 5, and we added Reference 13 in section 5.3.1 note "The fluorescence of the MOT is collected by a lens with spatial angle of about 10^{-4} rad. The loading phase atom number can be calculated by the method in Reference 13.". Ref.13 describes how to estimate the atom number from the photodetector signal.

2. "Section 3.2.2 discussed channels 2 and 3 of bias field coils and Table 1 listed the temperature settings of Channels 1-5 of their lithium oven, but the bias field direction generated by each coil channel and the location of each oven channel were not provided."
Response: A picture of the oven with labeled coil positions is included in Figure 4 and the direction of the bias field is now included in the note in 6.2 "In order to generate an interacting Fermi gas, a bias magnetic field in the vertical direction is applied to tune the s-wave scattering length."

3. "The information of the optical dipole trap beams (e.g., their beam waists and the polarizations) should also be pretty useful, but was not listed."
Response: The beam waist and polarization of each beam is now included in the caption of Figure 8.

4. In the introduction section, it is stated that "the lowering scheme also decreases the collision rate of the atoms" and this method can evaporatively cool Fermi gases without a lowering scheme. Does it imply that this method leads to a higher collision rate and can thus cool Fermi gases more effectively than a lowering scheme? Some widely-used methods, e.g., magnetic field tilting trap (Phys. Rev. A 78, 011604 (2008)), can also provide a high collision rate. Therefore, it will be very helpful to compare this parametric modulation method with some widely-used methods, and clearly list the advantages of this modulation method in the introduction section of the manuscript.
Response: We will address this question from two perspectives. First, without requiring lowering the trap depth, parametric driving provides a possibility to enhance the collision rate. As shown in Equation 10 of reference 6, the collision rate is reduced as the power law of the trapping potential for a Fermi gas (which is also true for a Bose gas). By keeping the trap depth, the collision rate will be maintained. Second, in this paper as well as in the previous publication Reference 7, we did not implement the parametric cooling scheme to interacting (collisional) Fermi gas because it has some nontrivial thermalization effects observed. Instead, we demonstrate this protocol for cooling a noninteracting Fermi gas. The noninteracting Fermi gases have zero collision rate, it is impossible to show a higher collision rate effect for a noninteracting Fermi gas. For our current experiment, we cannot make a comparison with Phys. Rev. A 78, 011604 (2008), which works for interacting quantum gas and shows a good way to maintain the high collision rate by titling the trap with magnetic gradient. We agree with the referee that it is rather interesting to compare the parametric cooling scheme with other schemes if we could apply this method to the interacting gases in the future. However, this comparison is beyond the scope of the current protocol paper. For the current protocol paper, we want

to emphasize the basic idea and effectiveness of the parametric cooling that by using the anhamornicity of the trap, we can selective remove the high-energy atoms even for a noninteracting Fermi gas.

5. The authors stated that "We find that the cloud energy in the axial direction is significantly reduced by parametric modulation, preparing an ultracold Fermi gas with anisotropic energy distribution" in the abstract. However, this statement is not supported by the data in Fig. 5: i.e., Fig. 5 shows that E_x and E_z were very different when no modulation (t_m = 0) was applied, but the difference between E_x and E_z decreased after a parametric cooling (e.g., at t_m ~ 600 ms). Therefore, Fig. 5 indicates that the traditional lowering scheme could also generate energy anisotropy, and the parametric modulation partially diminished the energy anisotropy. This contradiction should be clarified.
Response: The referee is right. We realized this inconsistency. In our previous publication of Reference 7, the parametric process increases/generates the energy anisotropy. However, in this paper, as shown in Fig.9 (old version Fig.5), the anisotropy decreases from 1.8/1.2 to 0.9/1.2. This shows the parametric cooling is not only able to generate anisotropy (Ref 7) but also can diminish the anisotropy (this paper) depending on the initial condition. So we changed our abstract to "We observe that the cloud energy is changed in an anisotropic way, where the energy of the axial direction is significantly reduced by parametric driving". This statement emphasizes the change is anisotropic instead of saying the final effect is anisotropy. We also provide more discussion in the "REPRESENTATIVE RESULTS" section. We write "We find that parametric cooling changes the atomic cloud energy in an anisotropic way, in which the energy in the axial direction is below the Fermi energy while the radial one is still above the Fermi energy. It is noted that the initial unequal energies in axial and radial directions (Figure 9b) are generated by the fast trap lowering applied in section 6.3. After the parametric cooling, the axial direction energy is significantly reduced while the radial energy is barely changed. This result indicates the way that parametric cooling changes the cloud energy is anisotropic."

6. To make a clear comparison of the author's parametric modulation method to the lowering scheme, data taken after further lowering the trap depth to a value small than 0.01 U_0 without a modulation should be present. These new data will be helpful to compare the lowering scheme and the parametric modulation method when the system is kept at a similar energy, which can better show the advantage of the parametric modulation method.
Response: Same as the 4th point, we should emphasize that parametric cooling in this paper is implemented for a noninteracting Fermi gas, while the lowering the trap depth is implemented in the interacting regime. It does not make sense to make such a comparison. If we lowered the trap depth in the noninteracting regime, we did not see any cooling effect, the atoms lost and the absolute temperature decreased, but the E/E_F are unchanged.

7. A sentence in section 3.3.2, "start the second stage of evaporative cooling 30 ms after 2.3.1", is confusing.

Response: In the current version, section 6.3.2 is the old section 3.3.2. We changed the sentence to “After the first state evaporative cooling is finished, we wait 30 ms, and then start the second stage of evaporative cooling”. The first and second stage of evaporative cooling explained in the first note in 6.3. We write “A standard evaporative cooling is used to cool the fermionic atoms of ^{6}Li near the degenerate regime. The first stage of evaporative cooling is controlled by the pulse of the fiber laser and the second is controlled by the ODT AOM.”

8. Figure 4 indicates that the dipole trap remains at 0.01 U_0 during the imaging stage. However, Section 5.1.7 states that "Program the APG to release the atoms from the ODT by abruptly turning off the trapping beams". These two appear to be contradictory and confusing.
Response: The old step 5.1.7 now is step 7.1.2. "Program the APG to release the atoms from the ODT by abruptly turning off the trapping beams" is the correct description of the required action. The old Figure is wrong, which is corrected by our new timing figure (Figure 2).

9. It will be useful for the reader if all important equipments are listed in Table-of-Materials/Equipment, e.g., multiplexer circuit used in Section 2.4, photodetector used in Section 2.4.1, and the beam reducer shown in Fig. 3. In addition, some of the equipment listed in the table are not mentioned in the manuscript, e.g., Faraday isolator.
Response: We accepted the referee’s suggestion. The Table of Materials now includes more equipment, such as the photodetector, Faraday (optical) isolator, multiplexer, and the lenses used for the beam reducer.

Reviewer # 2:
No Comments

Best,
Le Luo
Indiana University-Purdue University Indianapolis (IUPUI)

Click here to access/download
Supplemental File (as requested by JoVE)
2 Laser locking.pdf